Available online at www.sciencedirect.com
ScienceDirect
Journal of Solid State Chemistry 181 (2008) 183–189
JOURNAL OF SOLID STATE CHEMISTRY
www.elsevier.com/locate/jssc

Continuous hydrothermal synthesis of nanometric $BaZrO_3$ in supercritical water

A. Aimable, B. Xin, N. Millot*, D. Aymes*

Institut Carnot de Bourgogne, UMR 5209 CNRS, Université de Bourgogne, 9 Avenue Alain Savary, BP 47870, 21078 Dijon Cedex, France

Received 10 September 2007; received in revised form 13 November 2007; accepted 14 November 2007
Available online 21 November 2007

Abstract

Nanocrystalline barium zirconate ($BaZrO_3$) was synthesized using a hydrothermal synthesis process working in supercritical conditions and in a continuous way. By this method, we succeeded in the continuous and rapid production of nanopowders. As a preliminary work three barium precursors have been investigated: barium hydroxide ($Ba(OH)_2$), barium acetate ($Ba(CH_3COO)_2$) and barium nitrate ($Ba(NO_3)_2$). Two of them ($Ba(CH_3COO)_2$ and $Ba(NO_3)_2$) led to the pure perovskite phase. Then an experimental design has been conducted in order to determine the influence of the experimental parameters on the crystallinity and the grain size of the final product.

Keywords: Powders-chemical preparation; Grain size; $BaZrO_3$; Supercritical water synthesis

1. Introduction

Nanostructured ceramic materials are particularly interesting because of their physical properties depending on grain size [1]. Moreover, surface energy allows stabilizing phases outside the usual limits and new materials, very innovative, can be obtained [2]. Soft chemistry routes, high-energy dry grinding and hydrothermal synthesis have been developed during the last decades in order to obtain nanometric powders [3,4]. Most often, these techniques are developed in batch reactors. Continuous synthesis technologies, allowing several tens of grams of nanoparticles per hour production, are then very interesting to be developed at industrial level. In this perspective, a continuous production prototype of hydrothermal synthesis in subcritical and supercritical water has been developed in our group [5–7]. Recent papers summarise the specific characteristics of supercritical fluid processes for material synthesis and processing [8–12]. Two key features have been found: formation of nanoparticles, and ability to control particle morphology. This technology has also the advantage of being easy to use compared to closed reactors, and to have a high productivity.

Barium zirconate ($BaZrO_3$) is an interesting material for the refractory industry. Indeed, it is a high melting ceramic material (mp $\approx$2600 °C) with extensive functional utility as an inert crucible material for reaction and sintering of superconductors [13]. $BaZrO_3$ could also be a dopant in $BaTiO_3$ matrix [14]. It has also been tested as a thermal barrier coating for supersonic jets [15] and for sensor applications at high temperature in H_2 containing atmosphere [16].

Conventionally, zirconates have been synthesized through solid-state reaction of zircon with carbonates, oxides or nitrate elements of group IIA. Ultrafine powders of ZrO_2 have been converted into $MZrO_3$ (M = Ba, Sr, Ca) by the batch hydrothermal method [17]. The co-precipitation/calcination method was also used [18]. $BaZrO_3$ nanoparticles with diameter in the range of 30–40 nm were synthesized by sol–gel process [19]. A urea-induced precipitation process led to $BaZrO_3$ nanoparticles with a diameter around 90 nm [20].

In a recent study, Kolen'ko et al. [21] have obtained nanocrystalline ZrO_2 (8–12 nm), amorphous $ZrO(OH)_2$ or microcrystalline $BaZrO_3$ (2–5 μm) powders, depending on

*Corresponding authors. Fax: +33 3 80 39 61 67.
E-mail addresses: nmillot@u-bourgogne.fr (N. Millot), daymes@u-bourgogne.fr (D. Aymes).

0022-4596/$ - see front matter © 2007 Elsevier Inc. All rights reserved.
doi:10.1016/j.jssc.2007.11.015

the synthesis conditions, by an hydrothermal route in supercritical conditions at 673 and 783 °C but in a batch reactor . A previous publication showed for the first time the synthesis of nanocrystalline $BaZrO_3$ using the continuous hydrothermal synthesis process, from barium nitrate ($Ba(NO_3)_2$) and $ZrO(NO_3)_2$, in strong basic conditions at 500 °C [5]. In this new paper, we investigated the preparation of $BaZrO_3$ powders with the same process but using three different barium precursors: barium hydroxide ($Ba(OH)_2$), barium acetate ($Ba(CH_3COO)_2$) and $Ba(NO_3)_2$. Then an experimental design has been developed in order to study the influence of different operating parameters and establish the optimal conditions for obtaining a pure crystalline perovskite phase with the smallest grain sizes.

2. Experimental procedure

2.1. Apparatus

The experimental apparatus used for these hydrothermal syntheses was a continuous process described in Fig. 1. In one stream was fed the metal salt solution containing Zr and Ba source materials. This reactive solution was pressurized and combined with a pre-heated water stream (and eventually a basic solution fed in a third way) in a mixing point just before the reactor, which led to a rapid heating and subsequent reaction. The reactor was an inconel serpentine with a length of 2 m and an inner diameter of 2.3 mm, which led to a very fast reaction (around 10 s) that depended on the pumps flows. After the reactor, the solution was rapidly quenched. Filters retained agglomerated particles that were added to the suspension obtained after the backpressure regulator.

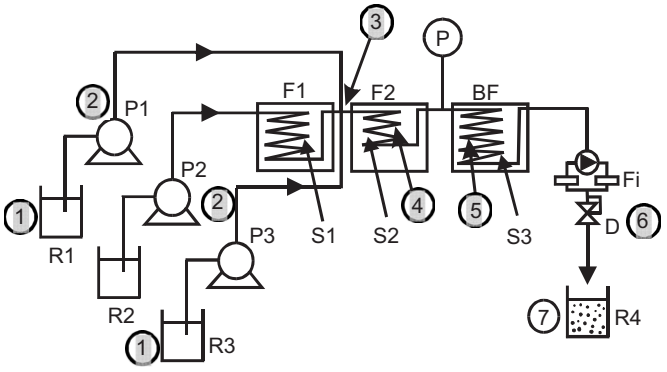

Fig. 1. Continuous hydrothermal synthesis process. Experimental protocol: (1) initial state cations in aqueous solution, (2) fast rise in pressure, (3) mixing point—rise in temperature, (4) conditions of synthesis (supercritical water medium), (5) cooling, (6) fall of pressure, (7) final state sol or suspension. Experimental set-up R1: cations solution, R2: water, R3: basic solution, P1, P2, P3: pumps of cramming, F1, F2: fluidized-bed owens, BF: cold bath, S1, S2: Inconel tubing, S3: stainless tubing, P: pressure gauge, Fi: filters on two parallel lines, D: back pressure regulator, R4: receiver.

2.2. Synthesis

The synthesis conditions are reported in Table 1. $ZrO(NO_3)_2 \cdot 6H_2O$ has been used as the Zr precursor. This solid could dissociate in a solution of nitric acid. Three different Ba precursors have been used, which are $Ba(OH)_2$, $Ba(CH_3COO)_2$ and $Ba(NO_3)_2$. With $Ba(CH_3COO)_2$ as well as $Ba(NO_3)_2$, a basic solution of sodium hydroxide was added. This was necessary in order to release OH^- ions for the neutralisation of protons; otherwise in the supercritical conditions the apparatus could suffer rapidly from acidic corrosion.

Reactions that occur in the apparatus are described as follows:

- Before the reactor, the dissolution of the precursors takes place (due to the high value of ε, the dielectric constant of water):

$$Ba(OH)_2 \rightarrow Ba^{2+} + 2OH^-, \quad (R1)$$

or

$$Ba(CH_3COO)_2 \rightarrow Ba^{2+} + 2CH_3COO^-, \quad (R1')$$

or

$$Ba(NO_3)_2 \rightarrow Ba^{2+} + 2NO_3^-, \quad (R1'')$$

$$NaOH \rightarrow Na^+ + OH^-, \quad (R2)$$

and

$$ZrO(NO_3)_2 \rightarrow ZrO^{2+} + 2NO_3^-. \quad (R3)$$

Table 1
Synthesis conditions of $BaZrO_3$ from different Ba precursors on the continuous hydrothermal synthesis process

Precursors		P (bar)	T (°C)	Residence time (s)	Reaction product	Heat-treated product
$ZrO(NO_3)_2$, $6H_2O$	0.025 mol L^{-1}	300	450	9	Amorphous	$BaZrO_3 + ZrO_2$
$Ba(OH)_2$	0.1 mol L^{-1}					
$ZrO(NO_3)_2$, $6H_2O$	0.025 mol L^{-1}	300	485	15	$BaZrO_3$	$BaZrO_3$
$Ba(CH_3COO)_2$	0.1 mol L^{-1}					
NaOH	1.5 mol L^{-1}					
$ZrO(NO_3)_2$, $6H_2O$	0.075 mol L^{-1}	300	450	31	$BaZrO_3$	$BaZrO_3$
$Ba(NO_3)_2$	0.3 mol L^{-1}					
NaOH	1.75 mol L^{-1}					

The heat treatment has been realised at 900 °C during 2 h under air atmosphere.

- After the mixing point, the precipitation in supercritical conditions takes place (due to the low value of ε):

$$ZrO^{2+} + Ba^{2+} + 2OH^- \rightarrow BaZrO_{3(s)} + 2H^+. \quad (R4)$$

Many experimental observations confirmed that the equilibrium of the reaction R4 is displaced to the formation of $BaZrO_3$, by both a great excess of hydroxide ions OH^- versus Ba^{2+} ($OH/Ba \geqslant 6$) to avoid the formation of ZrO_2 (reactions R8 and R9), and also by an excess of Ba^{2+} versus Zr^{4+} ($Ba/Zr = 4$). For instance, Lencka et al. [22] have calculated the thermodynamical stability diagram (composition-pH) for the hydrothermal synthesis of Perovskite phases ($BaTiO_3$, $PbTiO_3$, etc.) from precursors (Ba^{2+}, Ti^{4+}, OH^-) in aqueous solution. They show that the pH value must always be higher than 12. The study of Urek et al. [23] on the hydrothermal synthesis of $BaTiO_3$ shows that after the formation of $BaTiO_3$ nuclei from supersaturated solution, the aqueous suspension of formed nuclei is stable only when the pH value exceeds 13,

$$2H^+ + 2NO_3^- \rightarrow 2HNO_3. \quad (R5)$$

- In the cooler, the neutralisation of protons occurs (due to the high value of ε):

$$2HNO_3 \rightarrow 2\ H^+ + 2NO_3^-, \quad (R6)$$

$$2H^+ + 2OH^- \rightarrow 2H_2O. \quad (R7)$$

The by-product ZrO_2 can be easily formed by a two-step mechanism of hydrolysis and dehydration at high temperature and pressure if $[OH^-]$ is not high enough:

$$ZrO(NO_3)_2 + 2H_2O \rightarrow ZrO(OH)_2 + 2HNO_3, \quad (R8)$$

$$ZrO(OH)_2 \rightarrow ZrO_{2(s)} + H_2O. \quad (R9)$$

The suspensions obtained were centrifuged, washed with deionized water until neutral pH and freeze dried.

Portions of the powders obtained were thermally treated during 2 h at 900 °C under air atmosphere. This operation was realized in order to see if amorphous ZrO_2 would be formed during the synthesis.

2.3. Characterisations

All the characterisations were realised on freeze-dried powders.

Surface area measurements were performed using an AUTOSORB apparatus with N_2 adsorbing gas. The BET method is used to determine the surface area values from the isotherm of nitrogen adsorption.

All samples were characterised by X-ray diffraction (XRD) using a Siemens D5000 automatic powder diffractometer, with the $\lambda_{CuK\beta} = 1.39222$ Å radiation. The instrumental broadening correction was determined from a SiO_2 standard reference material from Brucker. Pseudo-voight peak profile analysis, using the Langford method [24,25] was performed to determine both the average crystallite size and crystallographic imperfections (a method including all the diffraction reflections for the calculation). The lattice parameter of the powders were deduced from XRD line positions using a least-squares refinement method.

Powders were all characterised by scanning electron microscopy (SEM). These experiments were conducted on a JEOL JSM-6400F electron microscope coupled with a LINK OXFORD energy dispersive X-ray analyser, which allows the determination of the metal ratio Ba/Zr. The mean grain size ϕ_{SEM} has been determined by analysing at least 50 grains.

3. Results and discussion

3.1. Synthesis from different barium precursors

XRD patterns of the powders obtained by hydrothermal synthesis on the continuous apparatus from different barium precursors (Table 1) are presented in Fig. 2. As shown in Fig. 2a, the synthesis conducted from $Ba(OH)_2$ led to an amorphous phase, which revealed a mixture of $BaZrO_3$ and tetragonal ZrO_2 after a heat treatment of 2 h at 900 °C under air atmosphere (Fig. 2b). In this case, if the amount of OH^- was increased by increasing the amount of $Ba(OH)_2$, the result was the same than for $Ba(CH_3COO)_2$ and $Ba(NO_3)_2$ precursors (see after). Nevertheless, the barium dihydroxide was often highly polluted by barium carbonate, and this impurity remained in the powder after filtration. It would be possible to avoid the formation of the barium carbonate, by freshly precipitation of barium hydroxide from barium oxide under a nitrogen atmosphere, and then transfer to the hydrothermal apparatus under a flow of nitrogen [26]. However, these operations are not adapted to an industrial process, which prefer using commercial reagents, and cannot afford working under nitrogen atmosphere. For the removal of $BaCO_3$, in industrial conditions, it is easier to wash powders at the

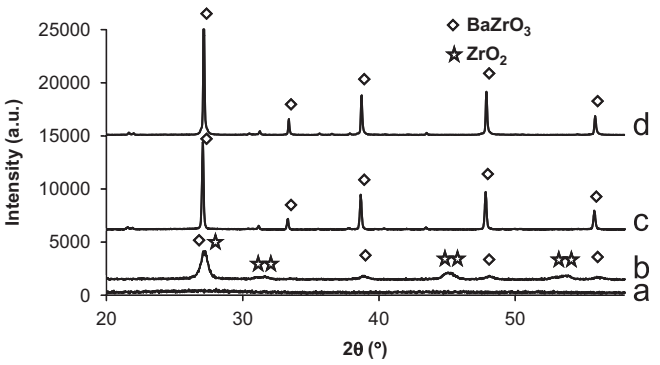

Fig. 2. XRD patterns of powders obtained hydrothermally in supercritical conditions depending on the Ba precursor: (a) reaction with $Ba(OH)_2$, (b) same powder heat treated 2 h at 900 °C under an atmosphere of air, (c) reaction with $Ba(CH_3COO)_2$ and (d) reaction with $Ba(NO_3)_2$. $\lambda_{CuK\beta} = 1.39222$ Å, $BaZrO_3$: 06–0399 ICDD card, ZrO_2: 50–1089 ICDD card.

end of the process with diluted acetic acid, after an aqueous washing, than using precursors exempt of $BaCO_3$ from the beginning. The synthesis needs very high pH values leading to the formation of $BaCO_3$ during both synthesis and recuperation steps.

From $Ba(CH_3COO)_2$ and $Ba(NO_3)_2$ precursors, the reaction products were well-crystallised $BaZrO_3$ powders with absence of the tetragonal ZrO_2 phase (Fig. 2c and d), even after a heat treatment of 2 h at 900 °C. The reflections not labelled are those of $BaCO_3$. As said previously, this phase appears when the suspension is in contact with air, and can be eliminated after an appropriate washing with diluted acetic acid. Others experiments show that if the ratio OH/Ba is equal to 2 (as for $Ba(OH)_2$), the synthesis leads also to an amorphous phase.

These powders were composed of small grains with a high specific surface area. This was confirmed by the SEM picture of the powder synthesised from $Ba(NO_3)_2$ presented in Fig. 3, which showed very small grains. This powder was well dispersed and homogeneous, with an average grain size of 100 nm. This value matched quite well the average particle size deduced from the specific area measurement, $S_{BET} = 10.4\,m^2\,g^{-1}$, which corresponded to a diameter of spherical grains of 92 nm. This relatively high value of specific surface enhanced the reactivity with CO_2 and lead, once more, to the carbonation of the $BaZrO_3$ powders even after the synthesis.

3.2. Experimental design applied to the $BaZrO_3$ synthesis

3.2.1. Definition of the experimental design

In order to study the influence of operating parameters on the $BaZrO_3$ synthesis, an experimental design has been conducted. The aim was to determine the optimal synthesis conditions for obtaining (i) pure perovskite powders, (ii) well-crystallised grains, and (iii) smallest grain sizes. The precursors used were $ZrO(NO_3)_2 \cdot 6H_2O$ and $Ba(NO_3)_2$ with a Ba/Zr ratio equal to 4. Five parameters have been studied: temperature (T), pressure (P), concentration of the reactants (Ba–Zr), concentration of the basic solution (OH) and residence time in the reactor (time). They have been set to two different values (a low value and a high value) that are given in Table 2. The selection of these parameters could seem quite narrow, but it was necessary to ensure the purity of the end product ($BaZrO_3$). Indeed, in others experiments which are not reported here, we have seen that at low temperature (below 380 °C), low pressure (below 230 bar), low Ba/Zr and OH/Zr ratios, and very short reaction time (a few seconds), a high percentage of amorphous ZrO_2 versus $BaZrO_3$ is obtained. Thus, this study was composed of $2^5 = 32$ syntheses, that are presented in Table 3.

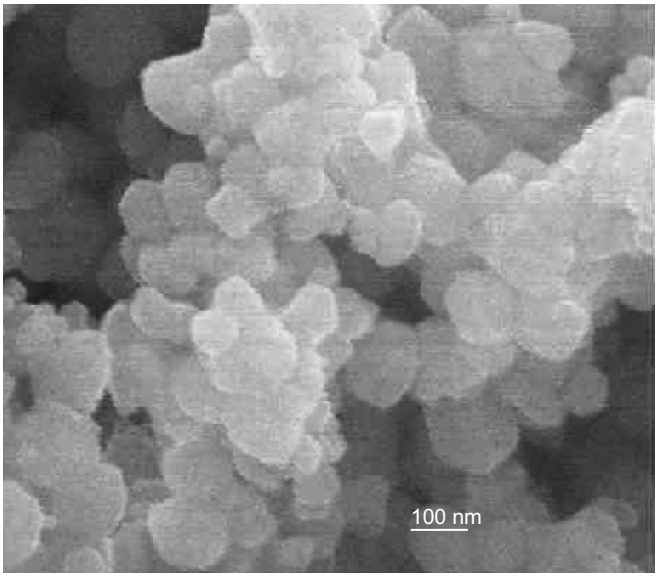

Fig. 3. SEM picture of the $BaZrO_3$ powder obtained hydrothermally in supercritical conditions ($P = 300$ bar, $T = 450$ °C) from the $Ba(NO_3)_2$ precursor.

3.2.2. Results and discussion

Results have been treated using the Taguchi method [27,28] and given in Table 4. The Taguchi method allows determining significant parameters by statistical calculations. One parameter can be considered as significant if its significance degree is more than 95%.

The perovskite phase has been directly obtained for the 32 syntheses, without annealing post-treatment. These powders were very well crystallised. Indeed, the XRD patterns clearly showed that the signal/noise ratio was excellent (see Fig. 4). Moreover, the Halder and Wagner method proved that these powders did not have any crystallographic defects (crystallographic defects rates were always between 0.05% and 0.14%, that means that there were no microdistortions, stacking faults, etc. in these powders).

The Ba/Zr ratio, determined by the energy dispersive X-ray analysis, was about 1.0 ± 0.2 for all the samples, which was consistent with the stoichiometry of the product $BaZrO_3$. There was no influence of the five parameters of the experimental design on this ratio.

Crystallite sizes, deduced from the Halder and Wagner method, are nanometric (Table 3). This was confirmed by SEM observations, which showed well dispersed and homogeneous nanometric powders. The average grain sizes deduced from SEM pictures were close to crystallite sizes deduced from XRD patterns, as shown in Fig. 4.

Table 2
Varying parameters in the experimental design conducted for the $BaZrO_3$ synthesis

	Low value (−1)	High value (+1)
Temperature (°C)	400	500
Pressure (bar)	250	350
Concentrations (mol L^{-1})	$[Zr^{4+}] = 0.025$	$[Zr^{4+}] = 0.075$
	$[Ba^{2+}] = 0.1$	$[Ba^{2+}] = 0.3$
[NaOH] (mol L^{-1})	1.0	2.0
Residence time (s)	10	17

Table 3
Conditions of the 32 experiments conducted in the experimental design, lattice parameter and crystallite sizes deduced from XRD patterns and SEM pictures

Trial	T	P	Ba–Zr	OH	Time	a (Å) ($\pm$0.001Å)	ϕ_{XRD} (nm) ($\pm$2 nm)	ϕ_{SEM} (nm) ($\pm$30 nm)
1	−1	−1	1	1	1	4.199	115	184
2	−1	1	1	1	1	4.214	98	184
3	−1	−1	−1	1	1	4.204	134	335
4	−1	1	−1	1	1	4.202	85	250
5	−1	−1	1	1	−1	4.208	121	155
6	−1	1	1	1	−1	4.205	82	176
7	−1	−1	−1	1	−1	4.205	67	158
8	−1	1	−1	1	−1	4.203	80	143
9	−1	−1	1	−1	1	4.207	120	155
10	−1	1	1	−1	1	4.198	100	162
11	−1	−1	−1	−1	1	4.202	101	151
12	−1	1	−1	−1	1	4.202	71	138
13	−1	−1	1	−1	−1	4.207	114	109
14	−1	1	1	−1	−1	4.230	131	129
15	−1	−1	−1	−1	−1	4.202	87	174
16	−1	1	−1	−1	−1	4.202	70	178
17	1	−1	1	1	1	4.198	122	172
18	1	1	1	1	1	4.198	66	125
19	1	−1	−1	1	1	4.198	221	182
20	1	1	−1	1	1	4.199	79	203
21	1	−1	1	1	−1	4.200	92	122
22	1	1	1	1	−1	4.193	75	96
23	1	−1	−1	1	−1	4.201	85	163
24	1	1	−1	1	−1	4.202	95	156
25	1	−1	1	−1	1	4.199	79	98
26	1	1	1	−1	1	4.197	86	112
27	1	−1	−1	−1	1	4.198	111	135
28	1	1	−1	−1	1	4.198	91	141
29	1	−1	1	−1	−1	4.199	65	81
30	1	1	1	−1	−1	4.198	95	76
31	1	−1	−1	−1	−1	4.200	95	99
32	1	1	−1	−1	−1	4.197	91	101

T: Temperature, P: pressure, Ba–Zr: concentrations of Ba^{2+} and Zr^{4+}, OH: concentration of NaOH, Time: residence time.
+1 and −1 corresponds, respectively, to the high and the low values of the parameter concerned in the experimental design (see Table 2).
Crystallographic defects rates were not reported since they were always between 0.05% and 0.14%, that means that there were no microdistortions, stacking faults, etc. in these powders.

Table 4
Results of the experimental design showing significant parameters (Yes), and their significance degree (>95% or >99%), and non-influent parameters (No), on the lattice parameter a, the particle size deduced from the Halder and Wagner method ϕ_{XRD}, the particle size deduced from the SEM pictures ϕ_{SEM} and from the BET surface ϕ_{BET}

Significative effect	Lattice parameter a	ϕ_{XRD}	ϕ_{SEM}	ϕ_{BET}
Temperature	Yes (>99%)	No	Yes (>95%)	No
Pressure	No	No	No	No
Reactant concentrations	No	No	No	No
[NaOH]	No	No	Yes (> 95%)	No
Residence time	No	No	No	No

Thanks to the Taguchi method, we were able to notice (Table 4) that the five parameters did not have any influence on the grain size deduced from both XRD and BET. Nevertheless, it appeared that temperature had a significant effect on the grain size deduced from SEM pictures (>95%). Larger particles were obtained at lower temperature: the average grain size was 129 nm at 500 °C, against 174 nm at 400 °C. Consequently, it seemed that higher temperature allowed a higher rate of germination, and a limited particles growth. The non-influence of the temperature on ϕ_{BET} might be due to the effect of the carbonate pollution (as previously mentioned, during storage and characterisation, powders continued to carbonate). Such remaining impurities, non-controlled in quantity, had a huge influence on the surface of the products (due to their very tiny grain sizes). The non-influence of the temperature on ϕ_{XRD} might be due, as for it, to some asymmetry of the XRD profils observed in some cases. This problem occurred when both temperature and base concentration were low (400 °C and 1 mol L^{-1}, respectively). In these conditions, some very tiny composition variations might occur and disturb the XRD line profile analysis.

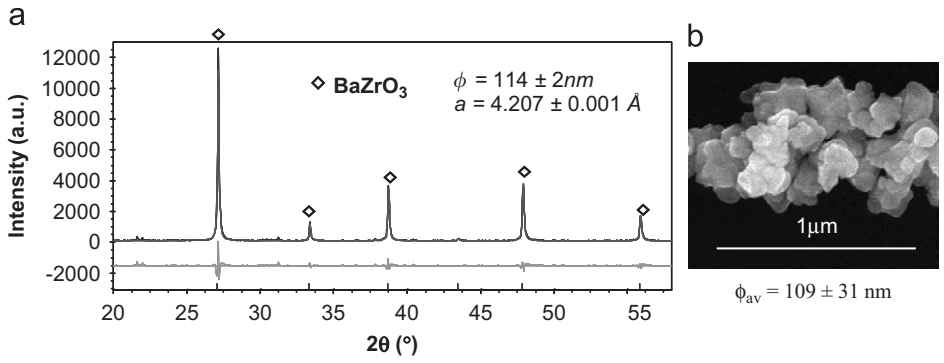

Fig. 4. (a) XRD pattern of one powder synthesised in the experimental design (trial 13), the crystallite size deduced from the Halder and Wagner method was 114 nm; (b) SEM picture of the same powder, the average grain size deduced from SEM picture was 109 nm. $\lambda_{CuK\beta} = 1.39222$ Å, $BaZrO_3$: 06–0399 ICDD card.

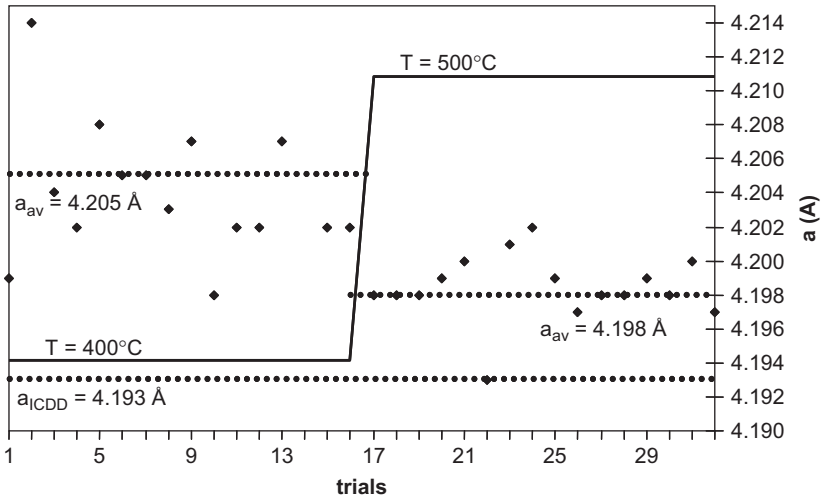

Fig. 5. Effect of the temperature on the lattice parameter of the powders synthesised in the experimental design.

The basic solution concentration has also a significant effect on the grain size deduced from SEM pictures (>95%). Indeed the average grain size was 175 nm when the basic solution concentration was 2 mol L^{-1}, whereas it was 127 nm when the basic solution concentration was 1 mol L^{-1}. Then a higher amount of basic solution favoured crystal growth. To obtain nanometric grains, it was then advised to conduct the synthesis with the minimum amount of NaOH.

This study showed also an important influence of the temperature on the lattice parameter. As shown in Fig. 5, the average lattice parameter of the powders synthesised at 500 °C was 4.198 ± 0.003 Å which was very close to the experimental value of the ICDD card 06–0399 ($a_{ICDD} = 4.193$ Å), whereas it was 4.205 ± 0.003 Å at 400 °C.

Such an important lattice parameter expansion (0.17%) cannot be related to the increase of grain size in the range 129/174 nm (ϕ_{SEM} for, respectively, 500/400 °C). Indeed, in the range 5–50 nm, for controlled materials, cell parameter appeared not to be linked to crystallite size ([29] and references therein). Moreover, a lattice parameter decrease was often observed when crystallite size increased [30]. In the case of the evolution published for $BaTiO_3$ [31], the lack of control of the hydroxide amount in these powders treated at different temperatures could explain the lattice parameter variation observed with the grain size evolution [32]. According to Tsunekawa et al. [33] the increase in ionicity of Ti ions was able to explain the anomalous lattice expansion measured in $BaTiO_3$ single nanoparticles with grain size decreasing.

In this new paper, by applying a higher temperature, some inserted compounds like OH^- could be released, which could explain the lattice parameter decrease of $BaZrO_3$.

The range of pressure was not large enough to observe any significant effect on the $BaZrO_3$ synthesis, neither for the reactant concentration and the residence time. For this last point, it could be assumed that in supercritical conditions, the reaction could occur in less than 10 s.

The reason of this lack of effect might be due to the selection of parameters which was rather narrow. These values have been chosen because in other experiments, not reported here, a high percentage of amorphous ZrO_2 versus $BaZrO_3$ was obtained at low temperatures (below 380 °C)

and low pressures (below 230 bar), with low ratios of Ba/Zr and OH/Zr, and very short reaction times (a few seconds). Nevertheless, this study illustrated a good stability of the device for an industrial point of view (for example, variations from 250 to 350 bar were allowed).

To conclude, this study exhibited the versatility of this process, which allowed the synthesis of pure and crystallised $BaZrO_3$, at a nanometric scale, in a large range of experimental conditions. Compared to "batch" processes, this process could be much more easily transferred to an industrial large-scale production, thanks to the very short reaction times (a few seconds), and its continuous running.

4. Conclusion

The preparation of $BaZrO_3$ has been conducted on a continuous hydrothermal synthesis process in supercritical conditions. Pure and nanocrystalline powders have been obtained from the reaction of $ZrO(NO_3)_2 \cdot 6H_2O$ with barium acetate or barium nitrate, in the presence of NaOH. An experimental design has been conducted in order to study the influence of some operating parameters on the crystallinity and the grain size of the as-synthesised materials. In the considered ranges, pure $BaZrO_3$ was always obtained, with grain sizes around 100 nm. Higher reaction temperatures allowed a higher purity of the samples, and smaller grain sizes. The main advantages of this process is its versatility, its productivity (thanks to the the continuous running), and the possibility of industrial-scale synthesis of well-dispersed $BaZrO_3$ nanoparticles in a wide range of experimental conditions.

References

[1] R.W. Siegel, E. Hu, D.M. Cox, H. Goronkin, L. Jelinski, C.C. Koch, M.C. Roco, D.T. Shaw, in: International Technology Research Institute, WTEC Panel Report on Nanostructure Science and Technology, 1998.
[2] N. Millot, D. Aymes, F. Bernard, J.C. Niepce, A. Traverse, F. Bourée, B.L. Cheng, P. Perriat, J. Phys. Chem. B 107 (2003) 5740.
[3] J. Gopalakrishnan, Chem. Mater. 7 (1995) 1265.
[4] M. Hirano, Recent Res. Dev. Mater. Sci. 3 (2002) 563.
[5] N. Millot, B. Xin, C. Pighini, D. Aymes, J. Eur. Ceram. Soc. 25 (2005) 2013.
[6] C. Pighini, D. Aymes, N. Millot, L. Saviot, J. Nanoparticle Res. 9 (2007) 309.
[7] N. Millot, S. Le Gallet, D. Aymes, F. Bernard, Y. Grin, J. Eur. Ceram. Soc. 27 (2007) 921.
[8] T. Adschiri, K. Kanazawa, K. Arai, J. Am. Ceram. Soc. 75 (1992) 1019.
[9] J.A. Darr, M. Poliakoff, Chem. Rev. 99 (1999) 495.
[10] J. Jung, M. Perrut, J. Supercrit. Fluids 20 (2001) 179.
[11] Y. Hakuta, H. Hayashi, K. Arai, Curr. Opin. Solid State Mater. Sci. 7 (2003) 341.
[12] F. Cansell, C. Aymonier, A. Loppinet-Serani, Curr. Opin. Solid State Mater. Sci. 7 (2003) 331.
[13] A. Erb, E. Walker, R. Flukiger, Physica C 258 (1995) 9.
[14] J.M. Herbert, Ceramic Dielectrics and Capacitors, Gordon and Breach Science Publishers, Philadelphia, 1985.
[15] R. Vassen, X. Cao, F. Trietz, D. Basu, D. Stover, J. Am. Ceram. Soc. 83 (8) (2000) 2023.
[16] H. Iwahara, T. Yajima, T. Hibono, K.H. Suzuki Ozaki, Solid State Ionics 61 (1993) 65.
[17] T.R.N. Kutty, R. Vivekanandan, S. Philip, J. Mater. Sci. 25 (8) (1990) 3649.
[18] J. Brzezinska-Miecznik, K. Haberko, M.M. Bucko, Mater. Lett. 56 (3) (2002) 273.
[19] M. Veith, S. Mathur, N. Lecerf, V. Huch, T. Decker, H.P. Beck, W. Eiser, R. Haberkorn, J. Sol Gel Sci. Technol. 17 (2000) 145.
[20] F. Boschini, B. Robertz, A. Rulmont, R. Cloots, J. Eur. Ceram. Soc. 23 (2003) 3035.
[21] Y.V. Kolen'ko, A.A. Burukhin, B.R. Churagulov, N.N. Oleinikov, A.S. Vanetsev, Inorg. Mater 38 (2002) 252.
[22] M.M. Lencka, R.E. Riman, Chem. Mater. 5 (1993) 61.
[23] S. Urek, M. Drofenik, J. Eur. Cer. Soc. 18 (1998) 279.
[24] J.I. Langford, 1992, in: Proceedings of The International Conference Accuracy in Powder Diffraction II, vol. 846, National Institute of Standards and Technology, Special Publication, p. 110.
[25] N.C. Halder, C.N.J. Wagner, Acta Crystallogr. 20 (1966) 312.
[26] R.I. Walton, F. Millange, R.I. Smith, T.C. Hansen, D. O'Hare, J. Am. Chem. Soc. 123 (2001) 12547.
[27] M.G. Vigier, Pratique des plans d'expériences, Méthode Taguchi, Les Editions d'Organisation, 1991.
[28] P.J. Ross, Taguchi Techniques for Quality Engineering, McGraw-Hill Professionnal, (Ed.), 1996.
[29] T. Belin, N. Guigue-Millot, T. Caillot, D. Aymes, J.C. Niepce, J. Solid State Chem. 163 (2002) 459.
[30] P. Ayyub, M. Multani, M. Barma, J. Phys. C, Solid State Phys. 21 (1988) 2229.
[31] G. Caboche, F. Chaput, J.P. Boilot, J.C. Niepce, Silicates Ind. 5 (1993) 103.
[32] Perrot-Sipple, F. Ph.D. Thesis, University of Burgundy, 1999.
[33] S. Tsunekawa, K. Ishikawa, Z.Q. Li, Y. Kawazoe, A. Kasuya, Phys. Rev. Lett. 85 (2000) 3440.